Proceedings of the
International Conference on Power Engineering-15
(ICOPE-15) November 30- December 4, 2015, Yokohama, Japan

Paper ID: ICOPE-15-1158

Supersonic air and wet steam jet using simplified de Laval nozzle

Takumi Komori*, Masahiro Miura*, Sachiyo Horiki* and Masahiro OSAKABE*
* Tokyo University of Marine Science & Technology
2-1-6Etchujima, Koto-ku, Tokyo 135-8533, Japan
E-mail: osakabe@kaiyodai.ac.jp

Abstract
Usually, Trichloroethane has been used for the de-oiling and cleaning of machine parts. But its production and import have been prohibited since 1995 because of its possibility to destroy the ozone layer. Generally for biological and environmental safety, the de-oiling should be done with the physical method instead of the chemical method using detergent or solvent. As one of the physical method, a cleaning by a supersonic wet steam jet has been proposed. The steam jet with water droplets impinges on the oily surface of machine parts and removes the oil or smudge. In the present study, the low-cost and taper-shaped nozzles were fabricated with an electric discharge machining. The jet behaviors from the taper-shaped nozzles were carefully observed by using air and wet steam. The non-equilibrium model of wet steam was proposed and compared with the experimental results. The spatial distribution of low density regions along the jet axis was considered to contribute the cleaning and de-oiling. However, the condensate generated with the depressurization of steam depressed the injected steam mass flow rate. Furthermore, the steam cleaning was conducted for the plastic coin and the good cleaning effect could be confirmed in spite of the short cleaning duration.

Key words : De-oiling, Cleaning, Machine parts, Physical cleaning, Supersonic wet steam, Taper-shaped nozzle

1. Introduction

Usually, Trichloroethane or CFC-113 has been used for the de-oiling and cleaning of machine parts. These cleaning solvents are inflammable, easy to evaporate, can percolate through complicated crevices and dissolve oily smudge. So the cleaning is not difficult technology if these solvents can be applied. But its production and import have been prohibited since 1995 because of its possibility to destroy the ozone layer. Other chemical solvents also have a possibility to destroy the ozone layer or promote the greenhouse effect, and some are harmful. Generally for biological and environmental safety, the de-oiling should be done with the physical method instead of the chemical method using detergent or solvent [Osakabe et al., 2009].

As one of the physical method, a de-oiling by the low-pressure flashing flow was investigated and verified by Horiki et al. (2000, 2001). In the present study, the supersonic wet steam jet was used instead of the flashing flow. The steam jet with water droplets impinges on the oily surface of machine parts and removes the oil or smudge. The supersonic steam jet can be generated with the convergent-divergent nozzle called as de Laval nozzle. The low-cost and taper-shaped nozzles were fabricated with an electric discharge machining. The conventional supersonic nozzles are usually fabricated with the laser machining and the surface is the three-dimensional. But the present nozzle with the electric discharging is simple taper as shown in Fig.1. The jet flow behavior was investigated in various conditions and the cleaning ability with the newly-fabricated tapered nozzles was experimentally confirmed.

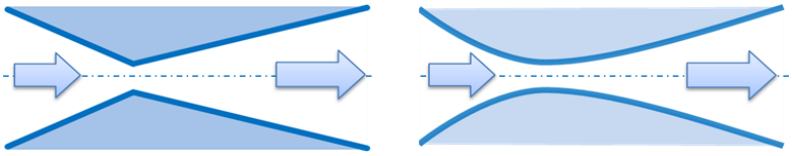

Fig.1 de Laval nozzle
(Left: electric discharge machining, Right: laser processing)

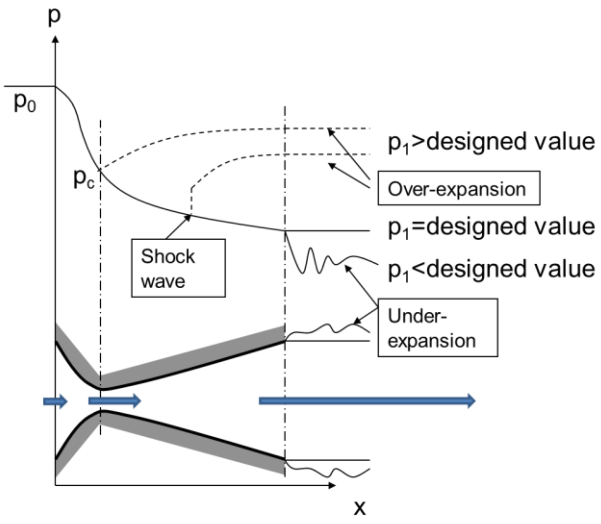

Fig.2 Under-expansion and over-expansion

2. Non-equilibrium model

Shown in Fig.2 is the pressure distribution in de Laval nozzle when the outlet pressure is changed. When the outlet pressure p_1 is smaller than the designed value, the expansion of flow cannot be completed in the nozzle and the sudden expansion at the outlet of nozzle takes place. This phenomenon is called as the under-expansion and the discharging behavior is unstable. It was considered that this instability can be used in the cleaning or de-oiling with the supersonic wet steam. When the outlet pressure p_1 is larger than the designed value, the expansion of supersonic flow continues and the sudden increase of pressure due to the shock wave takes place. After the shock wave, the supersonic flow becomes the subsonic flow and the pressure gradually increases to the outlet pressure. This phenomenon is called as the over-expansion and the energy loss cannot be negligible. It was considered that this energy loss and ensuing subsonic flow is not adequate for the cleaning or de-oiling with the wet steam.

In the case of wet steam, the super-saturation due to the delay of condensation takes place except the under-expansion and the over-expansion. The steam expands without the condensation and suddenly condensates at the impingement to surface to be cleaned. This non-equilibrium behavior contributes to the pressure fluctuation and the cleaning of machine parts.

The steam table gives the physical properties at the depressurized pressure. The entropy at the pressure p_1 is expressed as,

$$s_1 = x_1 s_{Gs} + (1 - x_1) s_{Ls} \tag{1}$$

Where x_1 is the quality, s_{Gs} and s_{Ls} is the enthalpy of saturated steam and water, respectively, at the depressurized pressure p_1. Considering the isentropic change, this entropy is equal to the inlet entropy s_0. So the quality can be obtained as,

$$x_1 = \frac{s_0 - s_{Ls}}{s_{Gs} - s_{Ls}} \tag{2}$$

By using the obtained quality, the specific volume and enthalpy at the equilibrium state after the depressurization can be given by

$$v_{e1} = x_1 v_{Gs} + (1 - x_1) v_{Ls} \tag{3}$$

$$h_1 = x_1 h_{Gs} + (1 - x_1) h_{Ls} \tag{4}$$

where v_{Gs} and v_{Ls} is the specific volume of the saturated water and steam, respectively, at the depressurized pressure. The enthalpy h_{Gs} and h_{Ls} is of the saturated water and steam, respectively, at the depressurized pressure. The outlet mass flux can be expressed with outlet specific volume v_1 and the enthalpy difference Δh between nozzle inlet and outlet.

$$G = \sqrt{2\Delta h} / v_1 \tag{5}$$

Assuming the isentropic change,

$$\Delta h = -\int_{p_0}^{p_1} v dp \tag{6}$$

It is considered that the rapid depressurization results as the non-equilibrium state due to the delay of phase change. Furthermore, the velocity difference of phase gives the smaller specific volume than the homogeneous specific volume. Considering the phase change delay and the velocity difference, the actual specific volume can be expressed as,

$$v = N\left(v_e - v_0\right) + v_0 \tag{7}$$

where N is the non-equilibrium parameter, v_e is the equilibrium specific volume, v_0 is the inlet specific volume of saturated steam. The factor is also used in the regulation of safety valve [Osakabe et al.(1996), Chiba et al.(2012), Kitagawa et al.(2014)]. The factor N=1 is the equilibrium state and 0 is the complete non-equilibrium state. By using the specific volume of Eq.(7), Eq.(6) becomes

$$\Delta h = N\left(h_0 - h_1\right) + \left(1 - N\right)v_0\left(p_0 - p_1\right) \tag{8}$$

The mass flux can be obtained with substituting the above enthalpy difference to Eq.(5). The non-dimensional mass flux can be expressed as,

$$G^* = \frac{G}{\sqrt{p_0 / v_0}} \tag{9}$$

The above equations are the non-equilibrium model using the steam table and commonly used to calculate the discharging mass flow from the safety valve.

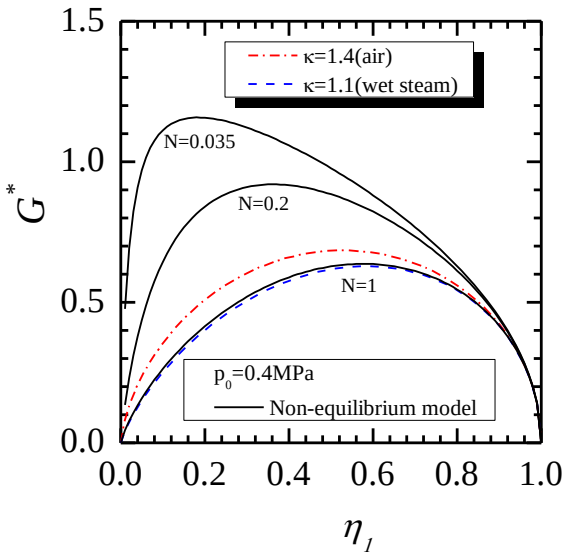

Fig.3 Effect of non-equilibrium

Shown in Fig.3 is the relation between the non-dimensional mass flux and the pressure ratio $\eta_1=p_1/p_0$ assuming the non-equilibrium factor N=1, 0.2 and 0.035 when the saturated steam at 0.4MP is discharged through the nozzle. The maximum peak of curve is the critical condition at the nozzle throat where the flow rate through the nozzle is limited. After the throat, the flow area of nozzle has to expand to become the mass flux corresponding to the outlet pressure ratio of design. The appropriate expansion is necessary to avoid the under-expansion or the over-expansion. The dashed or dot-dashed lines are calculated with the following equation assuming the ideal fluid [Osakabe, 2011].

$$G^* = \left[2\eta_1^{2/\kappa} \frac{1}{1-1/\kappa} \left(1-\eta_1^{1-1/\kappa}\right) \right]^{1/2} \tag{10}$$

For the ideal fluid, the sonic mass flux can be described as,

$$G_a^* = \left[\kappa \eta_1^{1+1/\kappa}\right]^{1/2} \tag{11}$$

The steam discharging behavior of N=1 can be approximately described with the ideal equation of specific heat ratio κ=1.1. When the non-equilibrium factor becomes smaller, the peak of curve becomes larger. The smaller factor indicates the strong non-equilibrium. The stronger non-equilibrium shifts the curve peak to the lower pressure ratio. If the under-expansion is expected to increase the cleaning effect of jet, the smaller pressure ratio is needed at the stronger non-equilibrium condition. When the outlet pressure is atmospheric pressure, the larger inlet pressure is necessary for the smaller pressure ratio.

Shown in Fig.4 is the relation between the outlet steam velocity and the pressure ratio $\eta_1=p_1/p_0$ assuming the non-equilibrium factor N=1, 0.2 and 0.035 when the saturated steam at 0.4MP is discharged through the nozzle. The smaller non-equilibrium factor results as the smaller velocity in spite of the larger mass flux shown in Fig.3. The larger mass flux is due to the larger density of discharging flow at the stronger non-equilibrium. When the nozzle outlet is the atmospheric pressure, the pressure ratio η_1 is 0.25 and the velocity becomes 500~700m/s.

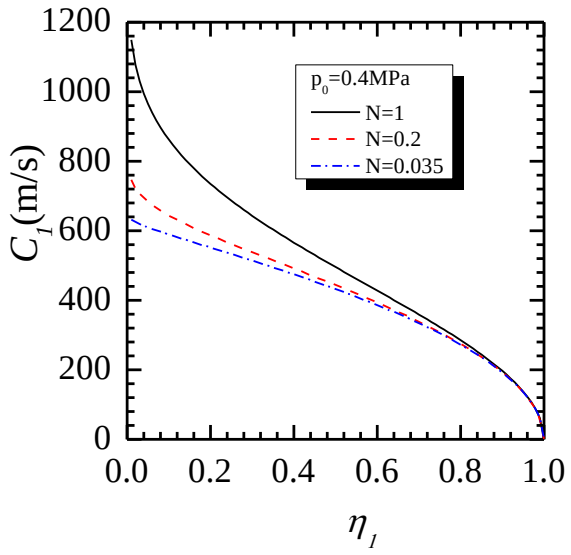

Fig.4 Discharging velocity dependent on non-equilibrium

3. Experimental apparatus and method

Shown in Fig.5 is the schematic of experimental apparatus. Air or steam is supplied to the nozzle from the tank after depressurized through the control valve. The tank is connected with steam boiler and air compressor, and can be pressurized up to 0.7 MPa. The steam flow rate through the nozzle is measured with the V-cone mass flow meter of

which measurement error is within ±2%. The air flow rate can be measured with the hot wire flow meter of which measurement error is within ±2%. The pressure is measured with pressure gages of which measurement error is within ±1.25 Pa. T-type sheath thermocouple of 1mm in diameter is used to measure the temperature. The total pressure of air jet was measured with the Pitot tube on the traverse apparatus.

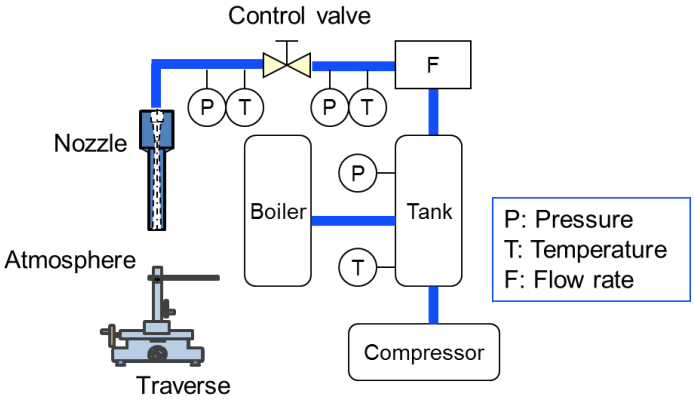

Fig.5 Experimental apparatus

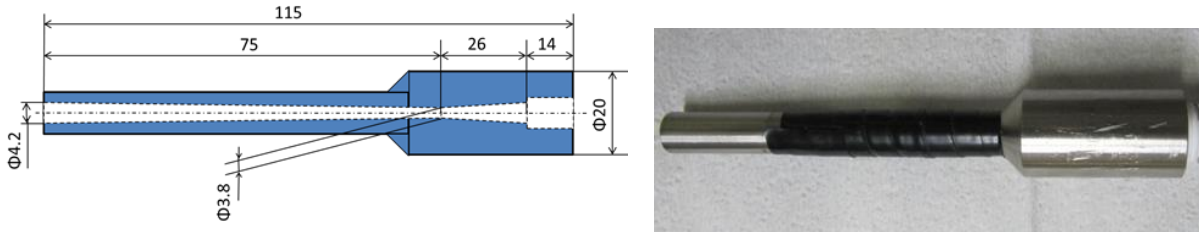

Fig.6 Drawings and picture of the de Laval nozzle

Shown in Fig.6 is the schematic of nozzle. The diameter of throat is 3.8mm and the outlet diameter is 4.2mm. So the expansion ratio is $(4.2/3.8)^2$=1.22 assuming the inlet air pressure of 0.4 MPa and the atmospheric outlet pressure.

The diameter of throat is the designed value on the drawing. So the actual diameter was estimated with the measured critical mass flow rate. Figure 7 is the relation between the measured critical mass flow rate W and the inlet pressure P_0. The critical mass flow rate depends linearly on the inlet pressure. The experimental data agrees well with the prediction with the throat diameter of 3.91mm instead of the designed diameter of 3.8mm. It was considered that the throat diameter was slightly enlarged with the surface polishing after the electric machining. The boundary layer effect at the throat can be also considered to exist due to the small diameter of nozzle.

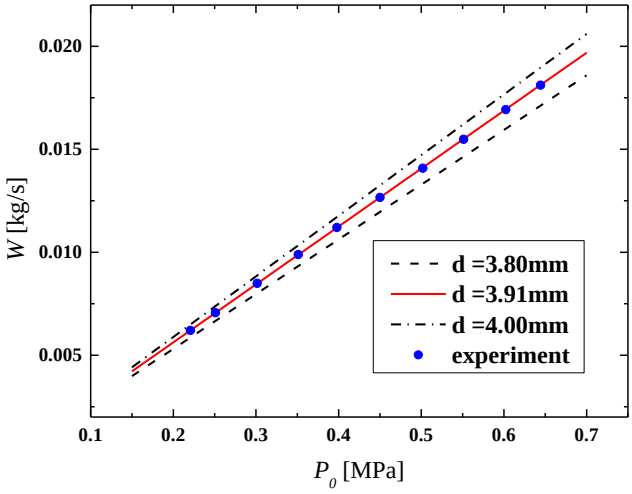

Fig.7 Critical mass flow rate dependent on throat diameter

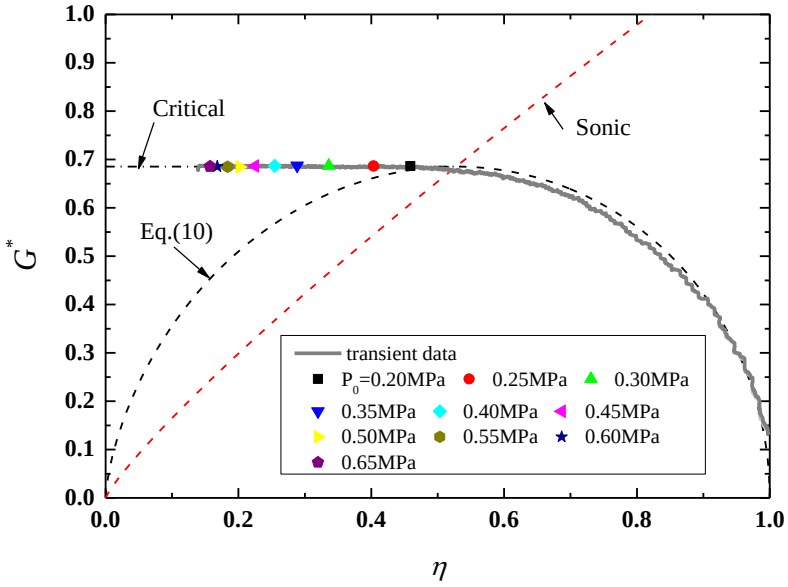

Fig.8 Non-dimension mass flux at the throat of the nozzle (d=3.91mm)

4. Experimental results

4.1 Air jet

In the air discharging experiments of present study, the temperature of air was approximately 20°C and the inlet pressure was controlled between 0.1 to 0.65 MPa. Basically the experiments were conducted with changing the discharging pressure step by step or with gradually decreasing the pressure due to the discharging flow from the isolated tank. The discharging jet behavior was recorded with video camera.

Shown in Fig.8 is the relation between the non-dimensional mass flux and the pressure ratio. The experimental data at the each inlet pressure and the transient data with decreasing the inlet pressure agree well with Eq.(10) of specific heat ratio κ=1.4. In the experiment, the actual throat diameter of 3.91mm was used to obtain the mass flux.

The mass flux at the nozzle outlet can be obtained as shown in Fig.9. When the experimental data crosses the parabolic curve of Eq.(10) at the pressure ratio of approximately 0.25, the discharging behavior changes from the over-expansion to under-expansion.

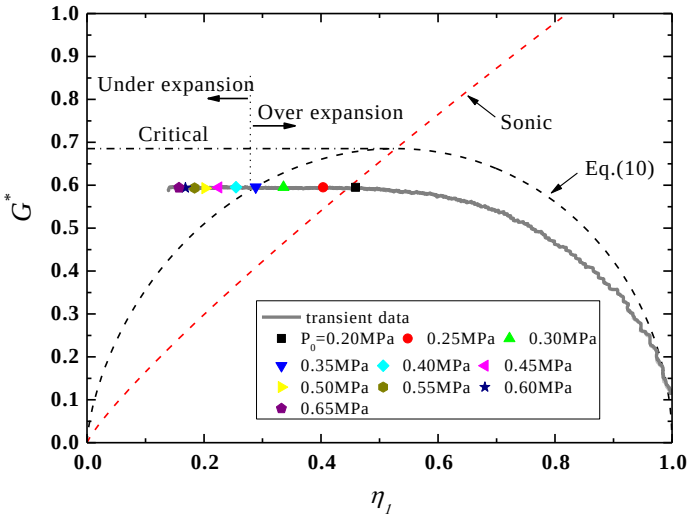

Fig.9 Non-dimension mass flux at the exit of the nozzle

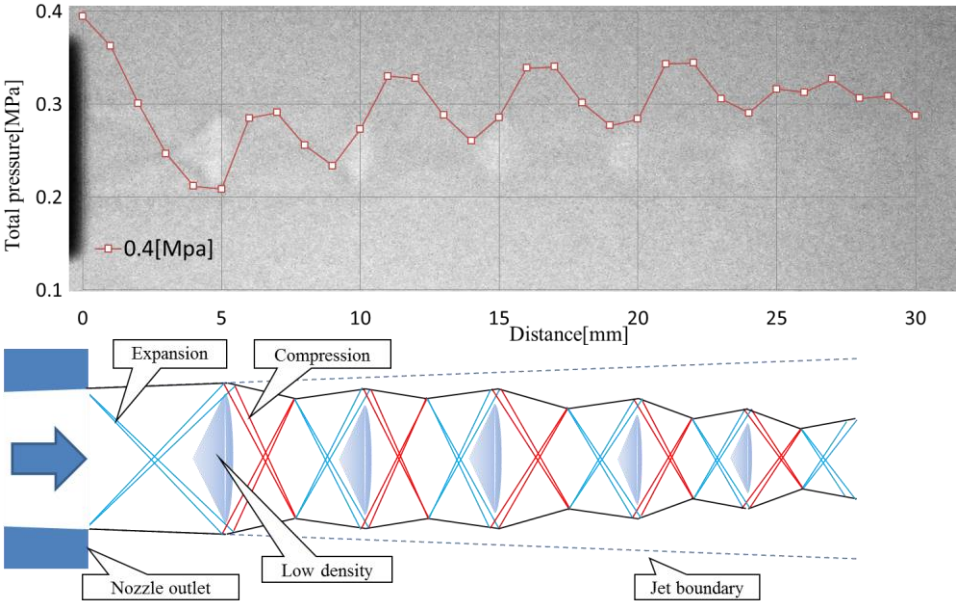

Fig.10 Expansion and compression wave in discharging jet

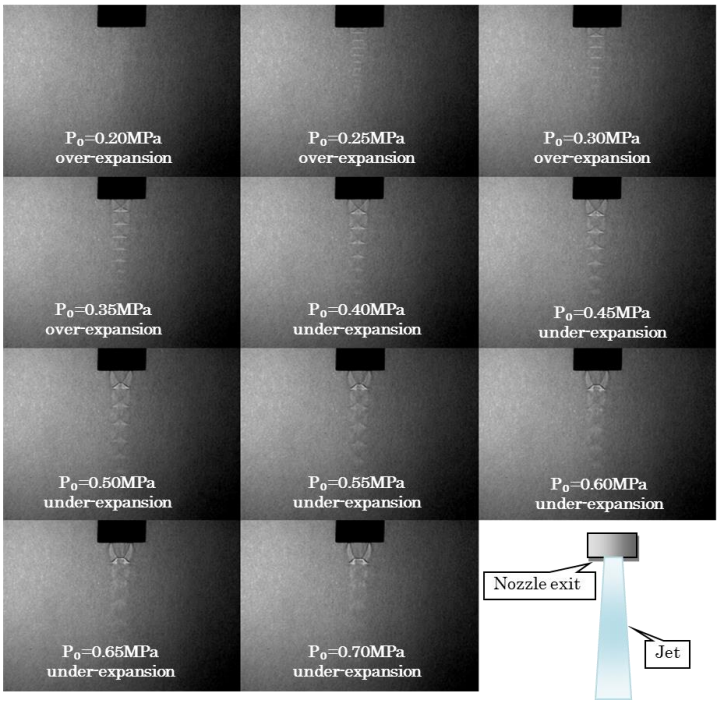

Fig.11 Visualization of pressure fluctuations in jet (P_0= 0.20 – 0.70MPa)

Shown in Fig.10 is the observed schlieren photograph and the corresponding total pressure distribution of typical under-expansion air jet flow. The several triangles of low density region along the jet axis can be observed in the photograph. The low density regions were generated with the expansion waves and the compression waves as shown in the lower illustration of Fig.10.

The schlieren photographs at the different inlet pressure are summarized in Fig.11. The train of low density regions can be recognized in the each photograph suggesting the pressure distribution along the jet axis. The clear train can be observed at the under-expansion jet of the inlet pressure larger than 0.4MPa. If the cleaning surface is put at the train region, the effective cleaning due to the interference with the expansion and compression waves can be expected.

The total pressure distributions along the jet axis are described on the schliren photograph as shown in Fig.12. The larger fluctuation of pressure can be observed at the under-expansion jet of the inlet pressure larger than 0.4MPa. When the inlet pressure exceeds 0.55MPa, the pressure fluctuation tends to decrease because the normal shock wave is generated just after the nozzle outlet. The supersonic flow changes to the subsonic flow after the normal shock wave called as the Mach disk. This subsonic jet cannot be expected for the effective cleaning.

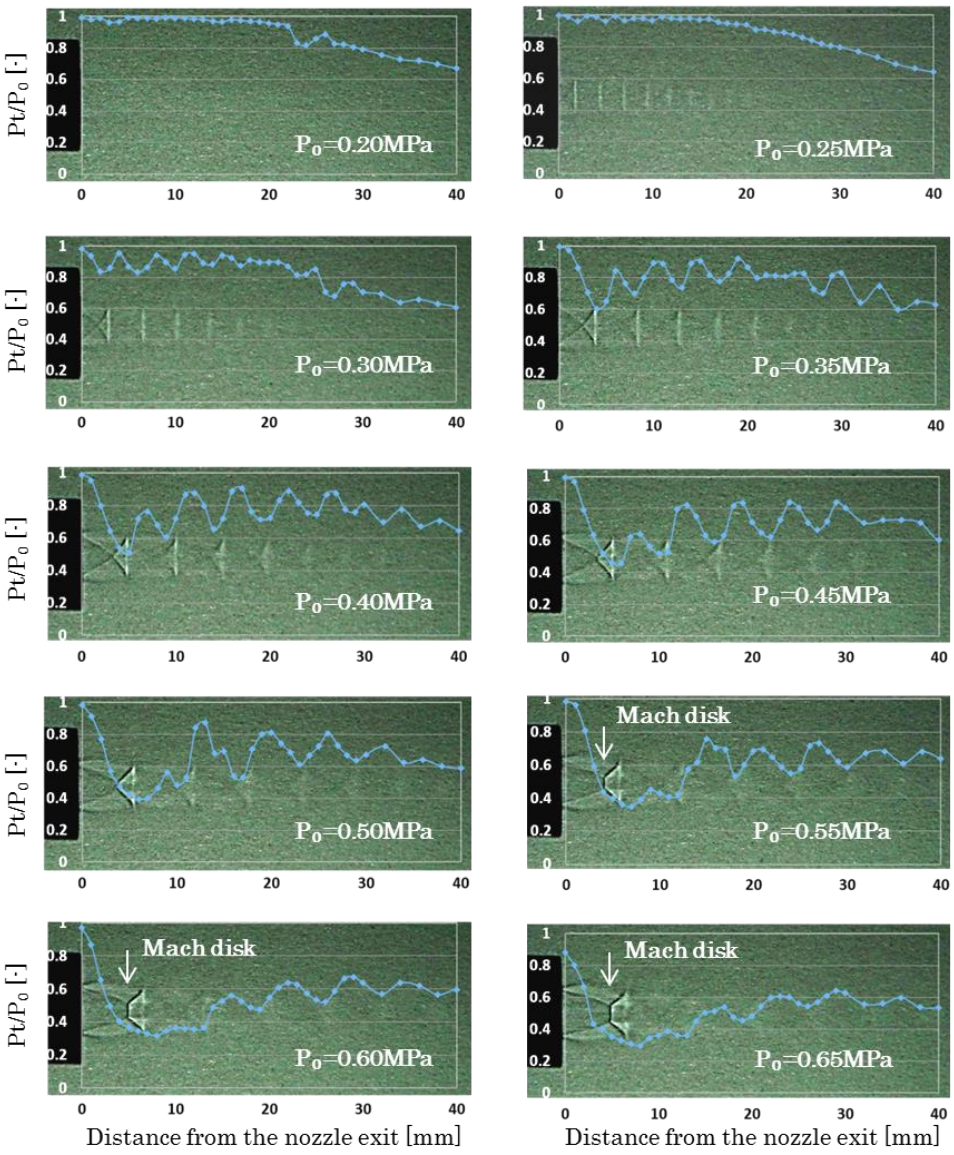

Fig.12 Visualization of pressure fluctuations in jet (P_0=0.20-0.65MPa)

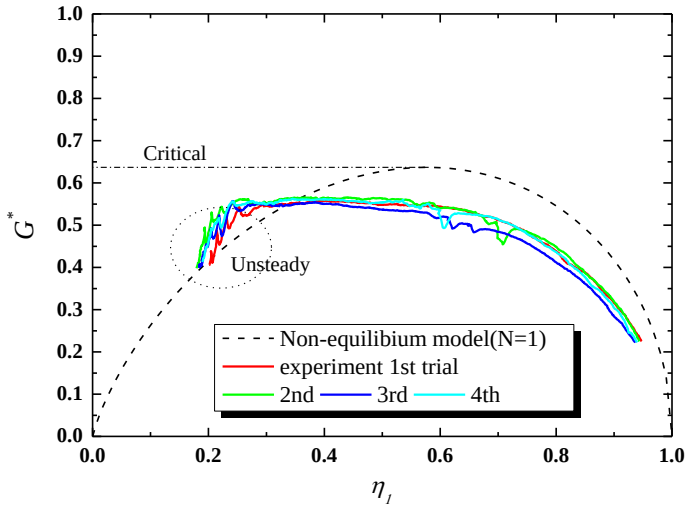

Fig.13 Non-dimension mass flux at throat of nozzle

4.2 Steam jet

In the steam discharging experiments of present study, the inlet pressure was set at 0.5 MPa and gradually depressurized with the discharging flow through the nozzle from the isolated steam tank. The discharging behavior was also recorded with video camera.

Shown in Fig.13 is the relation between the non-dimensional mass flux and the pressure ratio. The experiment started with the opening of the control valve at the smallest pressure ratio of 0.25 corresponding to the inlet pressure of 0.5MPa. When the steam began to flow through the nozzle, the unsteady flow rate was slightly low and increased with the oscillation. The experimental transient data with decreasing the inlet pressure is lower than the non-equilibrium model of N=1. In the experiment, the actual throat diameter of 3.91mm obtained with air experiment was used to calculate the mass flux. The smaller mass flux suggests the smaller throat diameter due to the condensate generated with the depressurization of wet steam.

If the throat diameter is reduced to 3.65mm from the actual value of 3.91mm, the mass flux becomes larger and agree well with the non-equilibrium model of N=1. So in that case, the thickness of condensate film is considered to be 0.13mm.

The steam jet was impinged on the acrylic plate with a small hole to measure the stagnation temperature and the total pressure. Shown in Fig.14 is the photograph of impinging experiment. From the rim of nozzle, the water film is discharging that suggesting the existence of water film in the inner surface of nozzle. The train of the low density regions as same as the air jet can be observed as shown in Fig.15. If the cleaning surface is put at the train region, the effective cleaning due to the interference with the expansion and compression waves can be expected.

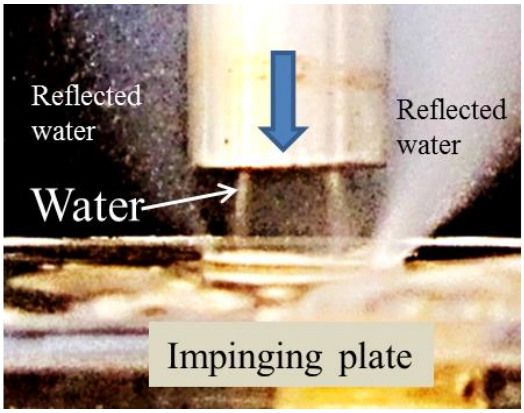

Fig.14 Photo of steam jet impinging on plate

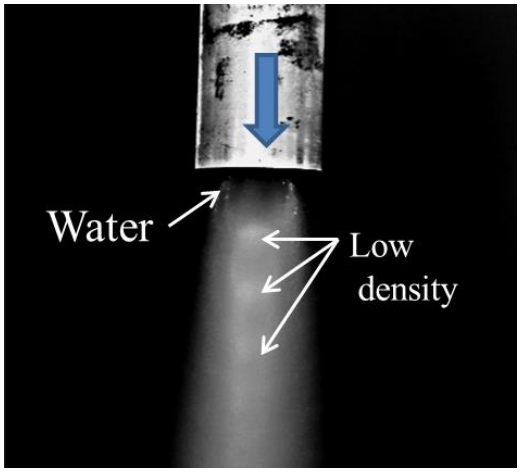

Fig.15 Photo of steam jet at nozzle exit

Shown in Fig.16 is the relation of stagnation pressure and the pressure ratio in the impingement experiment at the different distance from the nozzle outlet. When the impinging distance L is 5mm, the total pressure is approximately equal to the nozzle inlet pressure at the pressure ratio larger than 0.5 and significantly decreases with decreasing the

pressure ratio. The significant decrease is considered to be due to the energy loss due to the under-expansion behavior. When the impinging distance L is 50mm from the nozzle outlet, the total pressure linearly decreases with decreasing the pressure ratio. The inlet steam pressure of 0.5MPa becomes approximately 0.3MPa in the stagnation pressure at the impinging distance 50mm.

Shown in Fig.17 is the relation of stagnation temperature and the pressure ratio in the impingement experiment at the different distance from the nozzle outlet. When the distance L is 5mm, the stagnation temperature is approximately equal to the nozzle inlet temperature at the pressure ratio larger than 0.5 and gradually decreases with decreasing the pressure ratio. The moderate decrease is considered to be due to heat generation with the under-expansion behavior. When the distance L is 50mm far from the nozzle outlet, the stagnation temperature slightly decreases with decreasing the pressure ratio. The mixing with the ambient air of room temperature affects significantly at the far impinging distance. The inlet steam temperature of 400K becomes approximately 300K at the impinging distance 50mm.

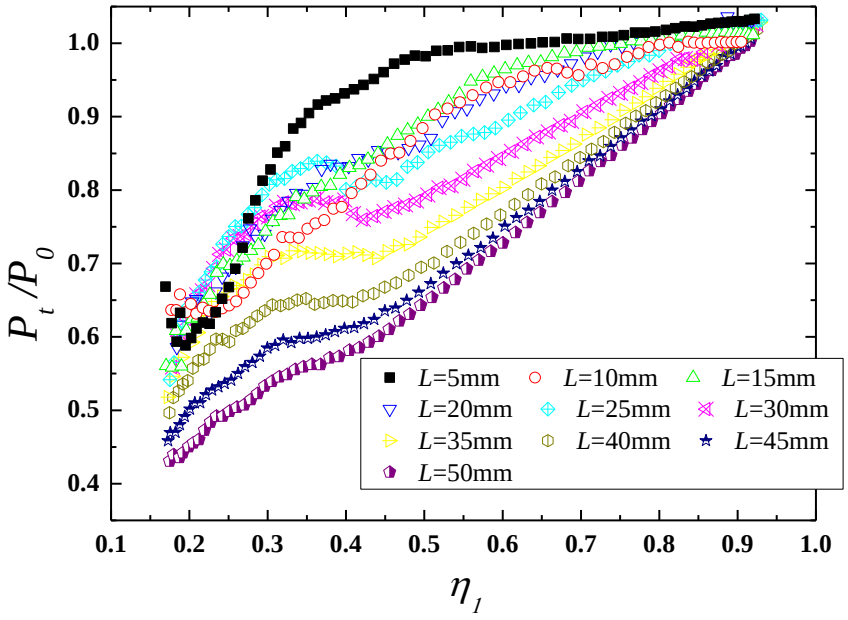

Fig.16 Relation of stagnation pressure and pressure ratio at different distance

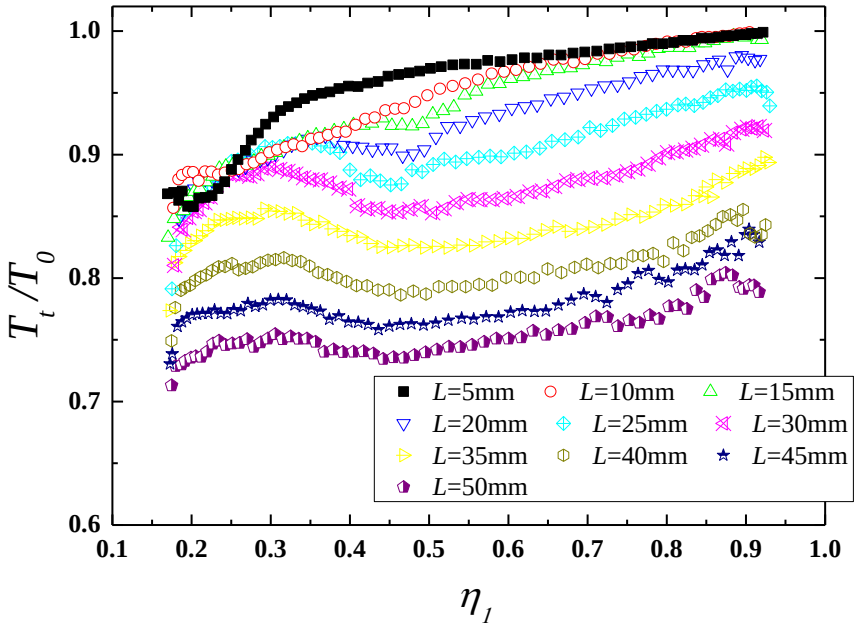

Fig.17 Relation of stagnation temperature and pressure ratio

4.3 Typical cleaning result

By using the tapered de Laval nozzle in the present study, the steam cleaning was conducted for the plastic coin shown in Fig.18. The nozzle inlet pressure was 0.4-0.5MPa and the distance from the nozzle outlet is 90mm. The inlet pressure assured the under-expansion of jet. The cleaning duration is only 5 seconds. The left photograph is before the cleaning and the right is after the cleaning. The coin before the cleaning was dirty with finger marks and the marks could be successfully removed with the supersonic steam jet. In spite of the short cleaning duration, the good cleaning effect could be confirmed.

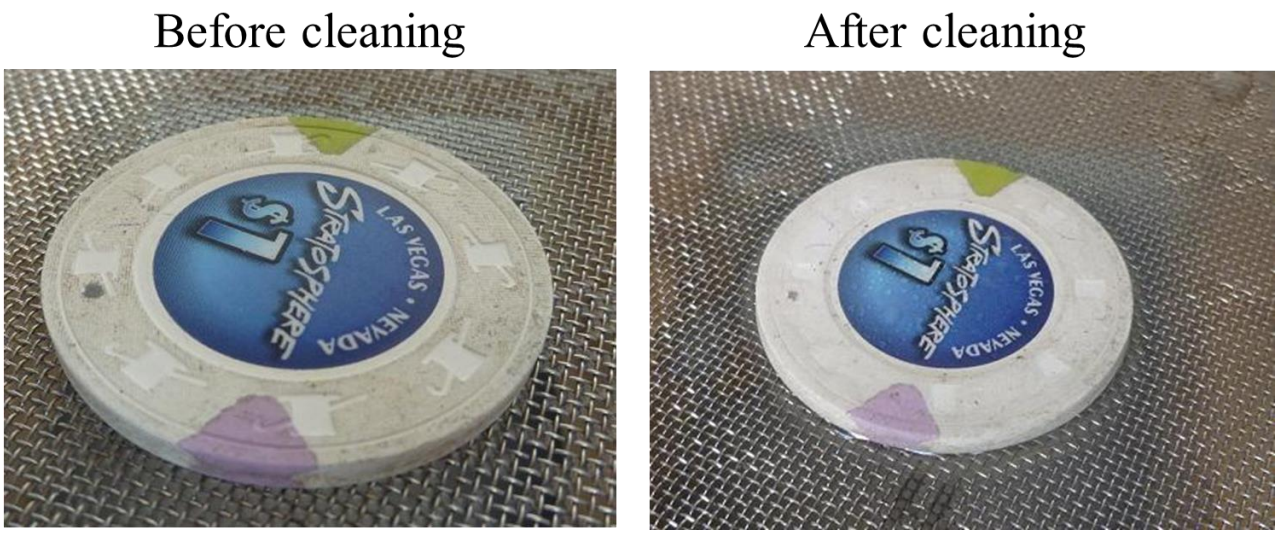

Fig.18 Typical cleaning result

5. Conclusions

As one of the physical method, a cleaning by a supersonic wet steam jet has been proposed. The steam jet with water droplets impinges on the oily surface of machine parts and removes the oil or smudge. In the present study, the low-cost and taper-shaped nozzles were fabricated with an electric discharge machining. The followings are major results.

(1) The discharging behaviors from the taper-shaped nozzles were carefully observed by using air. The spatial fluctuation of pressure could be observed at the under-expansion jet of the inlet pressure larger than 0.4MPa. If the cleaning surface is put at the fluctuation, the effective cleaning due to the interference with the expansion and compression waves can be expected. When the inlet pressure exceeded 0.55MPa, the pressure fluctuation tended to decrease because the normal shock wave was generated just after the nozzle outlet. The supersonic flow changed to the subsonic flow after the normal shock wave called as the Mach disk. This subsonic jet could not be expected for the effective cleaning.

(2) The non-equilibrium model of wet steam was proposed and compared with the experimental results. The steam discharging behavior of the non-equilibrium factor N=1 can be approximately described with the ideal gas equation of specific heat ratio κ=1.1. When the non-equilibrium factor N becomes smaller, the peak of curve becomes larger. The smaller factor indicates the stronger non-equilibrium. The stronger non-equilibrium shifts the curve peak to the lower pressure ratio. If the under-expansion is expected to assure the cleaning effect of jet, the smaller pressure ratio is needed at the stronger non-equilibrium condition. When the outlet pressure is atmospheric pressure, the larger inlet pressure is necessary for the smaller pressure ratio.

(3) The discharging behaviors from the taper-shaped nozzles were carefully observed by using wet steam. The spatial distribution of low density regions along the jet axis was also observed in the wet steam jet and the interference with the expansion and compression waves was considered to be effective for the cleaning. However, the condensate generated with the depressurization of steam depressed the discharging steam mass flow rate.

(4) Finally, the steam cleaning was conducted for the plastic coin and the good cleaning effect could be confirmed in spite of the short cleaning duration.

Nomenclature

C	velocity	(m/s)
d	throat diameter	(m)
G	mass flux	(kg/m^{2}s)
h	enthalpy	(J/kg)
Δh	enthalpy difference	(J/kg)
h_{LG}	latent heat	(J/kg)
N	non-equilibrium factor	(-)
p	pressure	(Pa)
Δp	pressure difference	(Pa)
s	entropy	(J/kgK)
T	temperature	(°C)
v	specific volume	(m^3/kg)
x	quality	(m)
W	mass flo*w* rate	(kg/s)
η	pressure ratio	(-)
κ	specific heat ratio	(-)

Subscript

0	inlet
1	outlet
a	sonic
e	equilibrium
s	saturated
t	stagnation
G	gas
L	liquid

References

Chiba, N., Kikkawa, K. and Osakabe, M., “Discharging flow behavior from disk-type flow contraction”, J. of Marine Engineering Society of Japan, 47(3), pp.58-63, (2012).

Horiki, S. and Osakabe, M., Cleaning and de-oiling of machine parts with low-pressure flashing flow, Proc. of ISME (Tokyo), 97-100, (2000).

Horiki, S. and Osakabe, M., Cleaning and De-oiling of Machine Parts with Low-pressure Flashing Flow, Proc. of the 2001 IJPGC (New Orleans), CD-ROM, (2001).

Kitagawa, Y., Horiki, S. and Osakabe, M., Non-equilibrium discharging flow from safety valves, Proceedings of the 15th International Heat Transfer Conference, IHTC-15, August 10-15, 2014, Kyoto, Japan, IHTC15-9810, (2014).

Osakabe, M. and Isono ,M., “Effect of valve lift and disk surface on two-phase critical flow at hot water relief valve”, Int. J. Heat and Mass Transfer, Vol.39, No.8, pp.1617-1624, (1996).

Osakabe, M., Horiki, S. and Ishihara, D., De-oiling ability of low pressure flashing water cleaner, Proc. of ICOPE-09 (Koube), (2009).

Osakabe, M., Fluid dynamics for engineers, Asakura Pub. Co., (2011). (in Japanese)